Journal of Organometallic Chemistry, 359 (1989) 115–125
Elsevier Sequoia S.A., Lausanne – Printed in The Netherlands

Stereochemical course of hydrogen addition to bis[(*S*,*S*)-2,3-bis(diphenylphosphino)butane]iridium(I). Crystal structure of dihydrogen bis[(*S*,*S*)-2,3-bis(diphenylphosphino)butane]-iridium(I) tetrafluoroborate

John M. Brown, Phillip L. Evans, Peter J. Maddox and Kevin H. Sutton
Dyson Perrins Laboratory, South Parks Rd. Oxford OX1 3QY (Great Britain)
(Received April 20th, 1988)

Abstract

Addition of H_2 to bis(*S*,*S*)-2,3-bis(diphenylphosphino)butaneiridium(I) tetrafluoroborate gives a single stereoisomer, whose crystal structure has been determined. Crystal data for $C_{56}H_{58}BF_4IrP_4$: orthorhombic space group, $P2_12_12_1$, a 12.157 (3) b 22.586 (6) c 20.226 (5) Å, $Z = 4$; the structure was refined to $R = 0.061$ and $R'_w = 0.081$ for 5090 unique reflections ($(I) > 3\sigma(I)$). The structure is compared with that of other hexacoordinate bis-biphosphine chelate complexes, and it is concluded that the stereospecificity of the hydrogen addition is steric in origin.

Introduction

Despite extensive efforts expended to establish the mechanism of asymmetric hydrogenation, the precise origin of enantioselectivity is not understood [1]. The rate-determining step involves addition of H_2 to a square-planar enamide complex (the one disfavoured at equilibrium). One source of complexity is the fact that four possible diastereomeric dihydrides may be formed in this addition step [2], and the preferred pathway is undefined since the initial product is converted into an alkylrhodium hydride too rapidly for its observation by NMR. Some recent theoretical papers on the addition of H_2 to square-planar complexes suggest that the transition-state occurs quite late along the reaction coordinate, with hydrogens equidistant from the metal [3]. The activation barrier is normally low, however [4], and therefore the transition-state structure can be dependent on local steric and electronic factors.

In an earlier study on the *cis–trans* isomerisation of bis (biphosphine)dihydroiridium cations, which occurs intramolecularly [5], we were intrigued to observe that H_2 addition to bis[(*S*,*S*)-2,3-bis-(diphenylphosphino)butane]iridium cation (**1**) ap-

0022-328X/89/$03.50

parently gives one of the two possible diastereoisomers of dihydride product **2a** or **2b**. During several days in solution at ambient temperature this rearranges to the *trans*-isomer. At the time it was considered that the stereospecificity of the addition step might reflect some discriminatory factor relevant to asymmetric hydrogenation (e.g. differential torsional strain development in the chelate backbone on clockwise versus anticlockwise twisting) [6], and this prompted us to determine the absolute configuration of **2**. The results are reported below.

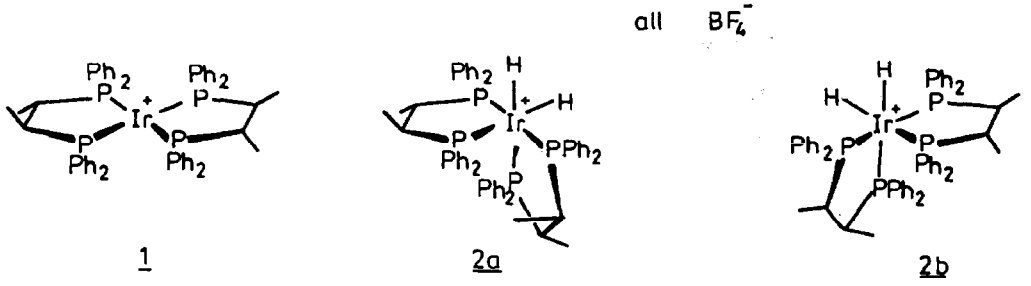

Results and discussion

A solution of complex **1** prepared as previously described [5], was dissolved in CD_2Cl_2 and exposed to H_2 at $-70\,^{\circ}C$. The reaction was monitored by ^1H NMR spectroscopy. The iridium hydride signal first became apparent at $-45\,^{\circ}C$ as a characteristic AA′ part of an AA′MM′XX′ spin system approximating to a double quartet, $\delta -11.73$ J(HP) (*trans*) 107 Hz, J(HP) (*cis*) 15 Hz. The spectrum was

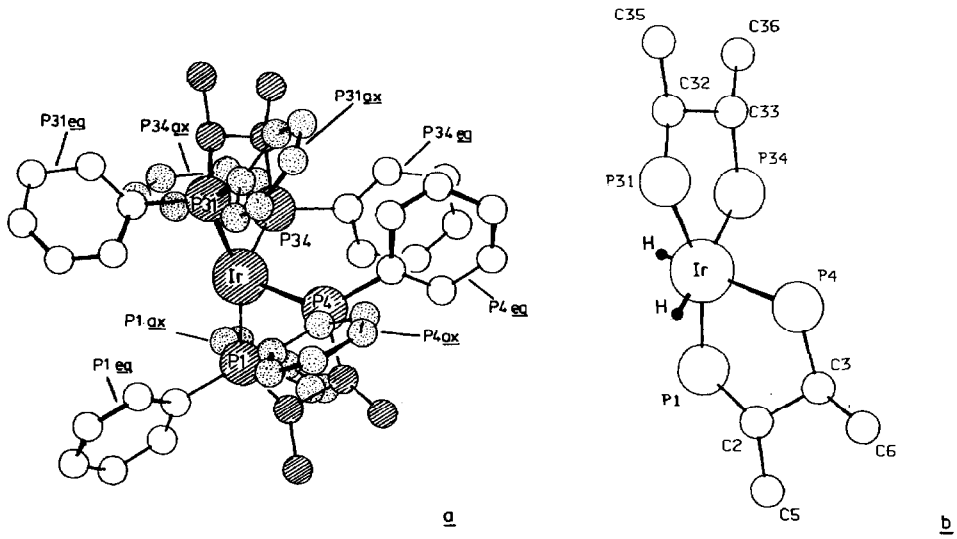

Fig. 1. The X-ray crystal structure of complex **2a**; (a) disposition of P–Ph rings chelate backbone indicated by ⊘ equatorial rings by ○ and axial rings by ◎. Atom connectivities (cf. Tables 1–3) P(1)–(C(7)–C(12)) Ph ax, P(1)–(C(13)–C(18)) Ph eq; P(4)–(C(19)–C(24)) Ph ax, P(4)–(C(25)–C(30)) Ph eq; P(31)–(C(37)–C(42)) Ph ax, P(31)–(C(43)–C(48)) Ph eq; P(34)–(C(49)–C(54)) Ph ax, P(34)–(C(55)–C(60)) Ph ax. (b) chelate backbone, with Ir–H imposed at octahedral positions.

essentially unchanged at 25 °C, consistent with the presence of a single stable complex. In a separate experiment this complex was isolated by adding the CH_2Cl_2 solution to hexane. Recrystallisation of the cream solid from acetone/hexane at 0 °C gave crystals suitable for X-ray analysis, as described in the Experimental section. Redissolution of a portion of the crystals in CD_2Cl_2 gave a solution whose NMR spectrum was identical to that originally observed, indicating that the crystals used for the X-ray study consisted of the complex obtained in solution.

Data collection and structure solution was carried out as described in the Experimental section. Hydrogen ligands on iridium could not be located by Fourier

Table 1

Bond lengths for complex **2a**

Ir(1)–P(1)	2.310(4)	C(21)–C(22)	1.40(3)
Ir(1)–P(4)	2.369(5)	C(22)–C(23)	1.37(3)
Ir(1)–P(31)	2.315(4)	C(23)–C(24)	1.38(2)
Ir(1)–P(34)	2.355(5)	C(25)–C(26)	1.39(3)
P(1)–C(2)	1.84(2)	C(25)–C(30)	1.41(3)
P(1)–C(7)	1.81(2)	C(26)–C(27)	1.36(3)
P(1)–C(13)	1.82(2)	C(27)–C(28)	1.36(4)
P(4)–C(3)	1.89(2)	C(28)–C(29)	1.45(4)
P(4)–C(19)	1.83(1)	C(29)–C(30)	1.30(3)
P(4)–C(25)	1.81(2)	C(32)–C(33)	1.54(3)
P(31)–C(32)	1.83(2)	C(32)–C(35)	1.53(2)
P(31)–C(37)	1.82(2)	C(33)–C(36)	1.56(2)
P(31)–C(43)	1.82(2)	C(37)–C(38)	1.39(3)
P(34)–C(33)	1.87(2)	C(37)–C(42)	1.39(3)
P(34)–C(49)	1.79(2)	C(38)–C(39)	1.35(3)
P(34)–C(55)	1.84(2)	C(39)–C(40)	1.35(3)
C(2)–C(3)	1.51(2)	C(40)–C(41)	1.37(3)
C(2)–C(5)	1.53(2)	C(41)–C(42)	1.45(3)
C(3)–C(6)	1.53(2)	C(43)–C(44)	1.41(4)
C(7)–C(8)	1.41(3)	C(43)–C(48)	1.42(3)
C(7)–C(12)	1.39(3)	C(44)–C(45)	1.43(4)
C(8)–C(9)	1.37(3)	C(45)–C(46)	1.64(6)
C(9)–C(10)	1.35(4)	C(46)–C(47)	1.33(5)
C(10)–C(11)	1.35(4)	C(47)–C(48)	1.28(4)
C(11)–C(12)	1.36(3)	C(49)–C(50)	1.42(3)
C(13)–C(14)	1.37(2)	C(49)–C(54)	1.41(3)
C(13)–C(18)	1.40(3)	C(50)–C(51)	1.35(3)
C(14)–C(15)	1.34(3)	C(51)–C(52)	1.58(5)
C(15)–C(16)	1.45(3)	C(52)–C(53)	1.32(5)
C(16)–C(17)	1.42(3)	C(53)–C(54)	1.48(3)
C(17)–C(18)	1.35(3)	C(55)–C(56)	1.31(3)
C(19)–C(20)	1.36(2)	C(55)–C(60)	1.48(3)
C(19)–C(24)	1.40(3)	C(56)–C(57)	1.46(3)
C(20)–C(21)	1.40(3)	C(57)–C(58)	1.43(4)
		C(58)–C(59)	1.31(5)
		C(59)–C(60)	1.37(4)
		B(1)–F(1)	1.29(3)
		B(1)–F(2)	1.19(5)
		B(1)–F(3)	1.29(4)
		B(1)–F(4)	1.34(6)

Table 2

Bond angles for complex (2a).

P(4)–Ir(1)–P(1)	84.4(2)	C(22)–C(21)–C(20)	116.4(20)
P(31)–Ir(1)–P(1)	160.8(2)	C(23)–C(22)–C(21)	123.0(18)
P(31)–Ir(1)–P(4)	107.6(2)	C(24)–C(23)–C(22)	117.4(20)
P(34)–Ir(1)–P(1)	107.3(2)	C(23)–C(24)–C(19)	122.4(20)
P(34)–Ir(1)–P(4)	102.3(2)	C(26)–C(25)–P(4)	125.8(18)
P(34)–Ir(1)–P(31)	85.1(2)	C(30)–C(25)–P(4)	115.7(15)
C(2)–P(1)–Ir(1)	107.1(5)	C(30)–C(25)–C(26)	118.5(19)
C(7)–P(1)–Ir(1)	118.4(6)	C(27)–C(26)–C(25)	120.4(22)
C(7)–P(1)–C(2)	111.2(8)	C(28)–C(27)–C(26)	120.9(23)
C(13)–P(1)–Ir(1)	116.1(6)	C(29)–C(28)–C(27)	117.2(22)
C(13)–P(1)–C(2)	101.8(8)	C(30)–C(29)–C(28)	121.7(24)
C(13)–P(1)–C(7)	101.0(8)	C(29)–C(30)–C(25)	120.2(23)
C(3)–P(4)–Ir(1)	107.5(6)	C(33)–C(32)–P(31)	110.1(11)
C(19)–P(4)–Ir(1)	116.2(6)	C(35)–C(32)–P(31)	120.4(16)
C(19)–P(4)–C(3)	102.6(8)	C(35)–C(32)–C(33)	109.6(16)
C(25)–P(4)–Ir(1)	123.8(6)	C(32)–C(33)–P(34)	110.0(12)
C(25)–P(4)–C(3)	103.4(9)	C(36)–C(33)–P(34)	113.1(13)
C(25)–P(4)–C(19)	100.8(7)	C(36)–C(33)–C(32)	114.7(16)
C(32)–P(31)–Ir(1)	108.3(6)	C(38)–C(37)–P(31)	119.5(15)
C(37)–P(31)–Ir(1)	119.2(6)	C(42)–C(37)–P(31)	121.1(15)
C(37)–P(31)–C(32)	108.8(9)	C(42)–C(37)–C(38)	119.1(18)
C(43)–P(31)–Ir(1)	112.1(6)	C(39)–C(38)–C(37)	121.2(21)
C(43)–P(31)–C(32)	104.2(10)	C(40)–C(39)–C(38)	121.9(21)
C(43)–P(31)–C(37)	103.2(9)	C(41)–C(40)–C(39)	119.6(23)
C(33)–P(34)–Ir(1)	106.7(6)	C(42)–C(41)–C(40)	120.5(22)
C(49)–P(34)–Ir(1)	117.4(6)	C(41)–C(42)–C(37)	117.6(19)
C(49)–P(34)–C(33)	101.2(9)	C(44)–C(43)–P(31)	121.8(19)
C(55)–P(34)–Ir(1)	121.5(6)	C(48)–C(43)–P(31)	119.9(18)
C(55)–P(34)–C(33)	102.9(9)	C(48)–C(43)–C(44)	117.7(22)
C(55)–P(34)–C(49)	104.3(9)	C(45)–C(44)–C(43)	126.4(31)
C(3)–C(2)–P(1)	110.2(10)	C(46)–C(45)–C(44)	106.2(28)
C(5)–C(2)–P(1)	118.3(14)	C(47)–C(46)–C(45)	124.8(27)
C(5)–C(2)–C(3)	112.8(16)	C(48)–C(47)–C(46)	120.2(38)
C(2)–C(3)–P(4)	108.7(11)	C(47)–C(48)–C(43)	123.9(32)
C(6)–C(3)–P(4)	112.4(13)	C(50)–C(49)–P(34)	124.8(16)
C(6)–C(3)–C(2)	112.2(13)	C(54)–C(49)–P(34)	120.4(14)
C(8)–C(7)–P(1)	123.5(15)	C(54)–C(49)–C(50)	114.7(17)
C(12)–C(7)–P(1)	120.9(15)	C(51)–C(50)–C(49)	123.5(24)
C(12)–C(7)–C(8)	115.4(17)	C(52)–C(51)–C(50)	118.0(23)
C(9)–C(8)–C(7)	122.3(24)	C(53)–C(52)–C(51)	122.0(26)
C(10)–C(9)–C(8)	119.5(27)	C(54)–C(53)–C(52)	113.5(33)
C(11)–C(10)–C(9)	119.9(24)	C(53)–C(54)–C(49)	128.1(22)
C(12)–C(11)–C(10)	121.7(26)	C(56)–C(55)–P(34)	126.9(18)
C(11)–C(12)–C(7)	121.1(25)	C(60)–C(55)–P(34)	112.6(17)
C(14)–C(13)–P(1)	121.9(15)	C(60)–C(55)–C(56)	120.4(21)
C(18)–C(13)–P(1)	120.0(14)	C(57)–C(56)–C(55)	119.4(23)
C(18)–C(13)–C(14)	118.1(18)	C(58)–C(57)–C(56)	117.6(30)
C(15)–C(14)–C(13)	123.2(22)	C(59)–C(58)–C(57)	121.9(33)
C(16)–C(15)–C(14)	120.4(21)	C(60)–C(59)–C(58)	121.3(30)
C(17)–C(16)–C(15)	114.8(21)	C(59)–C(60)–C(55)	118.9(26)
C(18)–C(17)–C(16)	122.8(24)	F(2)–B(1)–F(1)	121.5(35)
C(17)–C(18)–C(13)	120.6(21)	F(3)–B(1)–F(1)	104.0(29)
C(20)–C(19)–P(4)	122.6(13)	F(3)–B(1)–F(2)	121.7(48)
C(24)–C(19)–P(4)	118.8(12)	F(4)–B(1)–F(1)	98.3(46)
C(24)–C(19)–C(20)	118.0(15)	F(4)–B(1)–F(2)	98.8(40)
C(21)–C(20)–C(19)	122.5(20)	F(4)–B(1)–F(3)	109.0(48)

Table 3

Fractional atom coordinates and temperature factors for complex **2a**

Atom	x/a	y/b	z/c	U_{iso}
Ir(1)	0.00685(5)	0.21817(3)	0.21502(3)	0.0271
P(1)	−0.1800(3)	0.1999(2)	0.2196(2)	0.0289
P(4)	−0.0473(4)	0.3142(2)	0.1810(2)	0.0313
P(31)	0.1918(4)	0.2074(3)	0.1904(2)	0.0373
P(34)	0.0673(4)	0.2349(2)	0.3241(2)	0.0354
C(2)	−0.248(1)	0.2569(8)	0.1689(8)	0.0220
C(3)	−0.202(1)	0.3175(7)	0.1853(9)	0.0275
C(5)	−0.373(1)	0.256(1)	0.164(1)	0.0489
C(6)	−0.250(2)	0.3660(9)	0.141(1)	0.0458
C(7)	−0.244(1)	0.1933(9)	0.3000(8)	0.0349
C(8)	−0.317(2)	0.236(1)	0.326(1)	0.0529
C(9)	−0.362(2)	0.231(2)	0.388(1)	0.0646
C(10)	−0.334(2)	0.184(2)	0.426(1)	0.0716
C(11)	−0.261(2)	0.144(2)	0.404(1)	0.0651
C(12)	−0.217(2)	0.148(1)	0.3424(9)	0.0496
C(13)	−0.226(1)	0.1321(8)	0.1801(9)	0.0298
C(14)	−0.319(2)	0.1026(9)	0.201(1)	0.0441
C(15)	−0.356(2)	0.053(1)	0.172(1)	0.0486
C(16)	−0.298(2)	0.028(1)	0.116(1)	0.0626
C(17)	−0.205(2)	0.061(1)	0.094(1)	0.0576
C(18)	−0.171(2)	0.1101(9)	0.1248(9)	0.0427
C(19)	−0.020(2)	0.3332(7)	0.0947(7)	0.0321
C(20)	0.006(2)	0.3892(9)	0.0749(9)	0.0551
C(21)	0.019(3)	0.405(1)	0.008(1)	0.0674
C(22)	−0.001(3)	0.359(1)	−0.0382(9)	0.0630
C(23)	−0.034(2)	0.304(1)	−0.0208(9)	0.0535
C(24)	−0.039(1)	0.291(1)	0.0459(7)	0.0368
C(25)	−0.004(2)	0.3817(7)	0.2220(7)	0.0357
C(26)	−0.074(2)	0.4227(9)	0.252(1)	0.0498
C(27)	−0.033(2)	0.4749(9)	0.275(1)	0.0646
C(28)	0.075(3)	0.489(1)	0.268(1)	0.0738
C(29)	0.148(2)	0.442(1)	0.245(1)	0.0723
C(30)	0.110(1)	0.393(1)	0.223(1)	0.0512
C(32)	0.267(1)	0.1993(9)	0.268(1)	0.0348
C(33)	0.221(1)	0.2419(9)	0.3205(9)	0.0320
C(35)	0.393(1)	0.202(1)	0.269(1)	0.0491
C(36)	0.277(2)	0.237(1)	0.390(1)	0.0507
C(37)	0.260(1)	0.2634(8)	0.1401(9)	0.0334
C(38)	0.231(2)	0.270(1)	0.074(1)	0.0470
C(39)	0.278(2)	0.311(1)	0.035(1)	0.0568
C(40)	0.353(2)	0.350(1)	0.059(1)	0.0633
C(41)	0.382(2)	0.347(1)	0.124(1)	0.0564
C(42)	0.333(2)	0.3032(9)	0.168(1)	0.0470
C(43)	0.220(2)	0.139(1)	0.146(1)	0.0450
C(44)	0.288(2)	0.094(1)	0.173(2)	0.0755
C(45)	0.309(2)	0.038(1)	0.144(2)	0.0910
C(46)	0.240(3)	0.036(1)	0.075(2)	0.0765
C(47)	0.177(3)	0.079(2)	0.052(2)	0.1089
C(48)	0.161(2)	0.126(1)	0.087(1)	0.0681
C(49)	0.052(2)	0.1755(9)	0.3821(8)	0.0365
C(50)	0.036(3)	0.183(1)	0.451(1)	0.0719
C(51)	0.033(3)	0.138(2)	0.494(1)	0.0693
C(52)	0.046(3)	0.073(2)	0.466(2)	0.0872
C(53)	0.054(2)	0.062(1)	0.402(2)	0.0814

Table 3 (continued)

Atom	x/a	y/b	z/c	U_{iso}
C(54)	0.059(2)	0.1162(9)	0.361(1)	0.0494
C(55)	0.026(2)	0.3013(8)	0.3703(8)	0.0358
C(56)	0.088(2)	0.347(1)	0.385(1)	0.0573
C(57)	0.040(3)	0.397(1)	0.421(1)	0.0610
C(58)	−0.073(3)	0.392(2)	0.441(2)	0.0826
C(59)	−0.130(3)	0.344(2)	0.431(2)	0.0795
C(60)	−0.088(2)	0.298(1)	0.395(1)	0.0613
B(1)	0.511(5)	0.391(2)	0.307(1)	0.0763
F(1)	0.516(2)	0.4257(8)	0.3579(8)	0.1195
F(2)	0.477(4)	0.3417(9)	0.312(2)	0.1684
F(3)	0.482(5)	0.425(2)	0.260(1)	0.2079
F(4)	0.618(4)	0.379(2)	0.302(2)	0.2549

difference maps and so were omitted from structure factor calculations. The resulting structure with Ir–H incorporated at the vacant octahedral coordination sites, is depicted in Fig. 1; for clarity the phenyl rings are omitted in Fig. 1b.

The configuration at iridium is Δ, and both CHIRAPHOS chelates are in the expected δ conformation with all methyl groups in equatorial positions [7]. Bond lengths and bond angles for the complexes are recorded in Tables 1 and 2; the chelate angles of 84.4 and 85.1° are in accord with values for structurally related five-ring chelates [8]. The IrP_4 fragment occupies four adjacent sites in a distorted octahedron, the *trans*-pair being associated with a bond angle of 160°. Phosphine–iridium bonds *trans* to hydrogen are 0.05 Å longer than their partners, in accord with a generally observed *trans*-effect [9].

Stereochemical analysis. The crystal structure demonstrates that addition of H_2 to complex **1** is stereospecific, generating a *cis*-dihydride complex with Δ configuration at iridium and δ conformation of both chelate rings. This requires that complex **2a** is formed rather than **2b**, showing the original pathway of H_2 addition to be as drawn. To establish the origin of the observed stereospecificity, a survey was undertaken of crystallographic information available on octahedral complexes of type $M(P_2)_2XY$, where P_2 is a biphosphine which forms five-membered chelates and X, Y two other ligands in *cis*-relationships.

In a seminal paper [10], Corey and Bailar analysed coordination geometries of bis- and tris-(ethylenediaminecobalt) complexes, and showed that in the more stable tris-complex, the C–C bonds of the chelate backbone are oriented parallel to the C_3 axis. A modification of this approach was employed (Fig. 2), whereby the four possible dihedral angles linking the C–C backbones were determined. In many cases the metal configuration and ligand conformation could be retrieved from the literature if published diagrams were sufficiently clear. Otherwise they were obtained via the Cambridge Crystallographic Data Base. In all cases dihedral angles were calculated by use of the CHEMX (Molecular Design Ltd., Oxford) molecular graphics package. The full stereochemical analysis thus obtained is recorded in Table 4.

There are three possible geometries available to the set of complexes, designated **A**, **B**, and **C** (Fig. 2). Each of these permits a pair of enantiomers. The first entry in Table 4 relates to the present structure determination, whilst entries 2–4 correspond

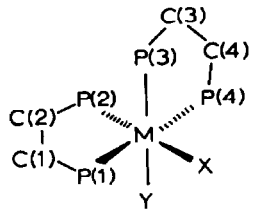

(a) C(1)—C(2)—C(3)—C(4)
(b) C(1)—C(2)—C(4)—C(3)
(c) C(2)—C(1)—C(3)—C(4)
(d) C(2)—C(1)—C(4)—C(3)

a

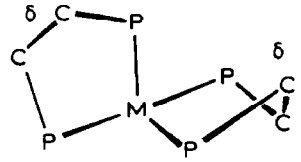

A: Δδδ (ΛλΛ)

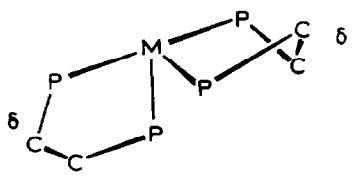

B: Λδδ (ΔλΛ)

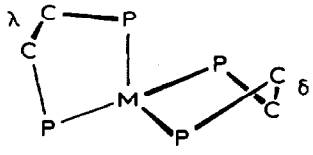

C: Δδλ (ΛλδΛ)

b

Fig. 2. (a) Definition of the sense of measurement of dihedral angles between the two chelate C–C bonds, (b) the three possible configurational isomers of an octahedral bis-chelate.

to model octahedral structures for the same complex created by using the CHEMX package and employing ligand coordinates from the rhodium (*SS* CHIRAPHOS) enamide complex structure [11]. It is clear that each geometry is associated with a distinct set of dihedral angles which differ from integral values because of slight deviation from C_2 symmetry in the enamide complex ligand. The remaining entries [12–22] are authentic crystallographic structures.

These literature structures are all based on achiral biphosphines, and so the configuration at the metal is arbitrary; they are all racemates (or conglomerates). They all fit into type **A** or type **C** stereochemistry and type **B** is lacking. Interestingly all dihydrides are of type **A** structure, and all dioxygen, disulphur, and related complexes are of type **C** structure. The difference in energy cannot be large in these cases, since ruthenium and osmium alkyl hydrides have different ligand conformations.

For an optically active, semirigid chelate complex such as **2** only the *Δδδ* and *Λδδ* configurations are permissible. It remains to be established why the former is formed and the latter is not; the result appears to be the expression of some general

Table 4

Stereochemical classification of octahedral bis-chelate complexes. Note the absence of any structures relating to type **B**

Entry	Complex	Ref.	Configuration at metal	Conformation by inspection	Dihedral angles [a] (degrees)	Structural Type [b]
1	Ir(*S*,*S*-chiraphos)$_2$H$_2^+$ BF$_4^-$	–	Δ	δδ	47.7, −133.2, −133.5, 43.4	**A**
Model structures						
2	Ir(*S*,*S*-chiraphos)$_2$H$_2^+$	–	Δ	δδ	64.4, −120.0, −120.0, 52.1	**A**
3	Ir(*S*,*S*-chiraphos)$_2$H$_2^+$	–	Λ	δδ	−168.8, 11.0, 11.0, −168.4	**B**
4	Ir(*S*,*S*-chiraphos)(R,R-chiraphos)H$_2^+$	–	Δ	δλ	116.2, −62.7, −69.0, 108.7	**C**
Literature structures						
5	Ir(dppe)$_2$H$_2^+$ B$_9$H$_{14}^-$	12	Λ	λλ	−56.7, 125.7, 125.7, −49.4	**A**
6	Ir(dppe)$_2$H$_2^+$ PF$_6^-$	13	Λ	–	−47.6, 134.2, 133.8, −42.3	**A**
7	Fe(dppe)$_2$H$_2$	14	Δ	[c]	46.0, −135.8, −135.2, 40.4	**A**
8	Fe(dppe)$_2$H$_2$	14	Δ	[c]	53.5, −127.3, −127.5, 49.2	**A**
9	Ru(dppe)$_2$H$_2$	15	Λ	λλ	–	**A**
10	Ir(dppe)$_2$O$_2^+$ PF$_6^-$	16	Λ	δλ	−111.2, 76.4, 68.0, −101.0	**C**
11	Rh(dppe)$_2$O$_2^+$ PF$_6^-$	16	Λ	δλ	−111.3, 76.1, 68.3, −101.1	**C**
12	Ir(dppe)$_2$Se$_2^+$ Cl$^-$	17	Λ	δλ	−113.2, 66.4, 71.1, −106.1	**C**
13	Ir(dppe)$_2$S$_2^+$ Cl$^-$	18	Δ	δλ	114.6, −64.5, −70.2, 107.6	**C**
14	Ir(dppe)$_2$(SO)$_2^+$ Cl$^-$	19	Δ	δλ	130.9, −47.6, −55.9, 122,5	**C**
15	(depe)$_2$IrSSCH$^+$ BPh$_4^-$	20	Λ	δλ	−109.6, 69.1, 74.6, −103.2	**C**
16	(depe)$_2$IrSSCPEt$_3^{2+}$ (BPh$_4^-$)$_2$	20	Δ	δλ	–	**C**
17	Mo(dppe)$_2$Cl$_2$	21	Δ	δλ	92.22, −87.64, −85.09, 92.03	**C**
18	Ru(dmpe)$_2$H(naphthyl)	22	Λ	[d]	−125.5, 53.6, 56.3, −122.1	**C**
19	Os(dmpe)$_2$H(naphthyl)	22	Λ	λλ	−64.9, 118.4, 120.2, −54.0	**A**

[a] The dihedral angles are listed in the order (a), (b), (c), (d) as defined by Fig. 2a. [b] See Fig. 2 for definition of structural types **A**, **B** and **C**. [c] No diagrams in literature. [d] Second chelate geometry unclear from inspection. dppe is 1,2-bis(diphenylphosphino)ethane, dmpe is 1,2-bis(dimethylphosphino)ethane, depe is 1,2-bis(diethylphosphino)ethane.

principle, since there are no examples of type **B** complexes in the literature. The explanation is probably steric rather than electronic. Molecular models indicate that the disfavoured $\Lambda\delta\delta$ configuration has a serious non-bonded interaction between ψ-equatorial phenyl rings which are *cis*-related in different chelates, the relevant P–C_{ipso} bonds are eclipsed. This interaction can be relieved by a conformational flip of one chelate ($\delta \rightarrow \lambda$), but in the present case this would produce a high-energy CHIRAPHOS structure with both methyl groups axial. In the $\Delta\delta\delta$ configuration the phenyl rings are better separated in space, with staggered P–C_{ipso} bonds in the region of closest contact.

Since the stereospecificity in the H_2 addition to complex **1** is steric in origin, it does not provide any insight into the face selectivity of asymmetric hydrogenation where comparable effects are absent. Future work will endeavour to define the extent of this face selectivity in more closely related models.

Experimental

All manipulations were carried out in freshly distilled solvents under in Schlenk apparatus. NMR spectra were recorded on a Bruker WH-300 (^{1}H) or AM-250 (^{31}P) instrument; for the latter chemical shifts are are given downfield relative to 85% H_3PO_4.

Bis[(S,S)-2,3-bis(diphenylphosphino)butane]iridium(I) tetrafluoroborate (1)

Following a procedure described by Brown, Dayrit and Lightowler [5], dichloromethane (4 ml) was added to a mixture of di-μ-chlorotetrakis(ethene)diiridium(I) (16.5 mg, 0.03 mmol) and (*S,S*)-2,3-bis(diphenylphosphino)butane (54 mg, 0.127 mmol). Ethene was evolved. The mixture stirred for 5 min then a solution of sodium tetrafluoroborate (250 mg, 2.3 mmol) in water (4 ml) was added. The mixture was vigourously stirred for 15 min, then the aqueous layer was removed by syringe, and the organic layer added to hexane (30 ml) with stirring. The bright orange precipitate was filtered off and dried in vacuo, to yield bis[(*S,S*)-2,3-bis(diphenylphosphino)butane]iridium(I) tetrafluoroborate (21.4 mg, 63%) m.p. 175 °C; δ(H) (300 MHz, CD_2Cl_2) 7.6–6.9 (40H, m, aromatic), 2.45 (4H, q, *J* 7.5 Hz, CH), 1.15 (12H, dd, *J* 7.5 and 15 Hz); δ(P) (101.2 MHz, CD_2Cl_2) 46.6 (S).

Dihydrogenbis[(S,S)-2,3-bis(diphenylphosphino)butane]iridium(I) tetrafluoroborate (2)

A solution of bis[(*S,S*)-2,3-bis(diphenylphosphino)butane]iridium(I) tetrafluoroborate (30 mg, 0.027 mmol) in dichloromethane (3 ml) in a small Schlenk tube at − 70 °C was three-times degassed and refilled with hydrogen by use of the hydrogenation apparatus. The solution was warmed to 25 °C, when the deep orange colour disappeared rapidly, then added to hexane (30 ml). The cream precipitate was filtered off and dried in vacuo. The solid was characterized as dihydrogenbis[(*S,S*)-2,3-bis-(diphenylphosphino)butane]iridium(I) tetrafluoroborate; δ(H) (300 MHz, CD_2Cl_2) − 11.73 (2H, dq, *J*(HP) 107, *J*(HP) 15.5 Hz, Ir–H); δ(P) (101.2 MHz, CD_2Cl_2) 29.3 (t, *J* 12.2 Hz), 19.3 (t, *J* 12.2 Hz). Single crystals for an X-ray structure determination were obtained by recrystallization from acetone/hexane at 0 °C.

Determination of the X-ray crystal structure of dihydrogen bis[(S,S)-2,3-bis(diphenylphosphino)butane]iridium(I) tetrafluoroborate (2)

Crystal Data. $C_{56}H_{58}BF_4IrP_4$, orthorhombic, space group $P2_12_12_1$, a 12.157(3), b 22.586(6), c 20.226(5) Å, U 5553.6 Å^3, $Z = 4$, T 290 K, μ(Mo-K_α) 7.84 cm^{-1}, $R = 0.061$, $R_w = 0.081$, GOF = 1.10 for 5090 unique observed ($(I) > 3\sigma(I)$) reflections.

Data were measured with graphite-monochromated Mo-K_α radiation on an Enraf–Nonius CAD-4 four-circle diffractometer. Reflections were scanned to a maximum of 50° (2θ) with a scan range of $\pm 1.0°$ min^{-1} depending on the intensity. Three standard reflections were monitored every 200 reflections and showed no decrease in intensity during data collection. Cell dimensions and standard deviations were obtained by least squares fit into 25 reflections ($26 < 2\theta < 28$). Reflections were processed with the CRYSTALS program to give 5090 unique observed ($(I) > 3\sigma(I)$) reflections. These were corrected for Lorentz, polarisation and absorption effects (by empirical methods). The structure was solved by Patterson methods and electron density Fourier synthesis and refined by block-matrix least squares. All non-hydrogen atoms were assigned anisotropic temperature factors and hydrogen atoms were assigned a common temperature factor and allowed to "ride" on their respective carbon atoms. The hydrogen ligands on the iridium could not be located by Fourier difference maps and so were omitted from the structure factor calculations. The largest peak on the final difference Fourier synthesis was 3.8 Å^3 in height, and was located near the iridium atom.

The structure was refined to final values of R 0.061, R_w 0.081 and GOF = 1.10. The maximum shift in the final cycle was 0.3σ. Computing was performed using CRYSTALS on a VAX11/750. Scattering factors were obtained from International Tables [23]. Final atomic positions with estimated standard deviations in parentheses are shown in Table 3 and bond lengths and angles in Tables 1 and 2. Lists of observed and calculated structure factors have been deposited in the Cambridge Database.

Acknowledgements

We thank SERC for studentships to PLE and PJM, the former on a CASE award with BP Research Centre. Dr. R.H. Jones was helpful in the early stages of collection and structure refinement. Johnson-Matthey afforded a generous loan of iridium salts. KHS thanks BP Research and Dr. S.G. Davies for postdoctoral support.

References

1 J. Halpern and C.R. Landis, J. Am. Chem. Soc., 109 (1987) 1746; J.M. Brown and P.J. Maddox, J. Chem. Soc. Chem. Commun., (1987) 1276.
2 P.A. Macneil, N.K. Roberts and B. Bosnich, J. Am. Chem. Soc., 103 (1981) 2273.
3 N. Kaga, C. Daniel, J. Han, X.Y. Fu and K. Morokuma, J. Am. Chem. Soc., 109 (1987) 3455 and refs. therein.
4 B.R. James in G. Wilkinson, F.G.A. Stone and E.W. Abel (Eds.), Comprehensive Organometallic Chemistry, Vol. 8, Ch. 51, p. 298, Pergamon, Oxford, 1982.
5 J.M. Brown, F.M. Dayrit and D. Lightowler, J. Chem. Soc. Chem. Commun., (1983) 414.
6 J.M. Brown and P.A. Chaloner in L.H. Pignolet (Ed.), Homogeneous Catalysis with Metal Phosphine Complexes, Ch. 4, p. 137 ff, Plenum Press, New York, 1984.

7 R.G. Ball and N.C. Payne, Inorg. Chem., 16 (1977) 1187.
8 For example, P. Albano, M. Aresta and M. Manassero Inorg. Chem., 19 (1980) 1069; E.P. Kyba, R.E. Davis, P.N. Juiri and K.R. Shirley, ibid., 20 (1981) 3616; H. Brunner, G. Vitulli, W. Porzio, and M. Zocchi Inorg. Chim. Acta, 96 (1985) 67, and ref. 11–22.
9 R.G. Teller and R. Bau, Struct. Bonding, 44 (1981) 1.
10 E.J. Corey and J.C., Bailar, Jr, J. Am. Chem. Soc., 81 (1959) 2620.
11 A.S.C. Chan, J.J. Pluth and J. Halpern, J. Am. Chem. Soc., 102 (1980) 5952.
12 N.N. Greenwood, W.S. McDonald, D. Reed and J. Staves, J. Chem. Soc. Dalton Trans., (1979) 1339.
13 T. Debaerdemaeker, Cryst. Struct. Commun., 6 (1977) 1.
14 E.B. Lobkovski, M.Y. Antipin, A.P. Borisov, V.D. Makhaev, K.N. Semenenko and Y.T. Struchkov, Koord, Khim., 6 (1980) 1267.
15 P. Pertici, G. Vitulli, W. Porzio and M. Zocchi, Inorg. Chim. Acta, 37 (1979) L52.
16 J.A. McGinnety, N.C. Payne and J.A. Ibers, J. Am. Chem. Soc., 91 (1969) 6301.
17 A.P. Ginsberg, W.E. Lindsell, C.R. Sprinkle, K.W. West and R.L. Cohen, Inorg. Chem., 21 (1982) 3666.
18 W.C. Bonds, Jr., and J.A. Ibers, J. Am. Chem. Soc., 94 (1972) 3413.
19 T. Debaerdemaeker, Cryst. Struct. Commun., 5 (1976) 765.
20 C. Bianchini, P. Innocenti, A. Meli, A. Orlandini and G. Scapacci, J. Organomet. Chem., 233 (1982) 233.
21 G. Pelizzi and G. Predieri, Gazz. Chim. Ital., 112 (1982) 381.
22 U.A. Gregory, S.D. Ibekwe, B.T. Kilbourn and D.R. Russell, J. Chem. Soc. A, (1971) 1118.
23 International Tables for X-Ray Crystallography, Kynoch Press, Birmingham, 1974, Vol. 4.